Fibers and Polymers 2018, Vol.19, No.6, 1318-1326
DOI 10.1007/s12221-018-8075-5

ISSN 1229-9197 (print version)
ISSN 1875-0052 (electronic version)

7Effects on Thermal and Ablative Properties of Phenolic Resin (Novolac) Blended Acrylonitrile Butadiene Rubber

Rashid Nawaz[1], Naghmana Rashid[1], Zulfiqar Ali[2], Asad U. Khan[2], M. Shahid Nazir[2], and Noaman Ul-Haq[2]*

[1]*Department of Chemistry Allama Iqbal Open University, Islamabad 44310, Pakistan*
[2]*Department of Chemical Engineering, COMSATS Institute of Information Technology, Lahore 53800, Pakistan*
(Received February 2, 2018; Revised March 9, 2018; Accepted March 31, 2018)

Abstract: In this work we investigated the ablative response and thermal properties of phenolic resin (PR) blended acrylonitrile butadiene rubber (NBR) composites. PR was added to NBR in the proportion of 0, 5, 10, 20, 30, 40 and 50 phr by means of two-roll laboratory mill. PR remarkably improved ablation resistance and thermal properties of NBR/PR composite. The linear and mass ablation rates reduced to 21.3 % and 26.1 % respectively. The char content deposition increased from 0.19 to 26.8 %. Char layer produced by PR, obviously reduced the erosion rate of the NBR/PR composite relative to neat NBR (without PR). Detailed morphological studies of the composite and post-test (ablation) microstructure of char revealed that higher loading of PR in the rubber composite produced dense char layer firmly intact to the substrate. Furthermore, thermal stability of the composite improved by 22-23 ºC, however, thermal conductivity of the composite slightly increased by 0.115 W/mK for 50 Phr of PR loading as compared to the neat.

Keywords: Phenolic resin (PR), Nitrile butadiene rubber (NBR), Ablative properties, Thermal properties, Morphological studies

Introduction

Rubber has got a unique position in engineering applications because of its distinctive properties like high extensibility, strength, energy absorption, and resistance to fatigue. Without reinforcement, rubber has limited applications. In aerospace industry, polymeric based ablative materials are widely used for thermal protection [1-3]. Ablative composites have outstanding capability to withstand oxidative environments at high temperatures, and play an important role in reducing the temperature rise. Selection of elastomer based ablative is made keeping in view the hypothermal environment being faced by an aerodynamic body. The performance of an ablative material mainly depends on two parameters i.e. ablation and thermal conduction through ablator [4,5].

Elastomers have low thermal conductivity as compared to the compounding ingredients. Nearly all additives increase thermal conductivity of the composite [6]. Properties of composites depend upon the nature of elastomer, filler, Elastomer-filler interaction and dispersion of filler in host matrix. Due to non-reactive and resistant to extreme environment, silicone rubber has been investigated with a variety of flame retarding materials like ZrC, ZrO_2, SiO_2, Magnesium Hydroxide, Multi-walled carbon nanotubes (MWNTs) and carbon fiber [7-9]. Ethylene propylene diene ter monomer rubber (EPDM) being a material with a low specific gravity, outstanding resistance to oxidation, shelf life and excellent low temperature properties has emerged as a novel material for diverse applications. EPDM filled with Kevlar, Polyphenylsilsesquioxane (PPSQ), Asbestos, Polysulfonamide pulp(PSA-pulp), $A1_2O_3$, $MgZrO_2$, Cr_2O_3, SiC, carbon powders and phenolic resin have greatly improved thermal and ablative efficiency [2,10-12]. Hydrogenated nitrile butadiene rubber (HNBR) composites filled with fumed silica, organically modified montmorillonite (OMMT) and expanded graphite (EG). HNBR/OMMT exhibited good resistance against flame [13]. Composites based on blends of NBR/PVC, SBR/Phenolic Resin, EPDM/NBR with various fillers displayed enhancement in ablative properties relative to the unblended polymer [13-15]. Silicone rubber based composites have been used extensively but it expands upon heating. Silicone & EPDM elastomers, show low resistance to oil absorption and swelling. On the basis of the engineering applications, acrylonitrile butadiene rubber (NBR) is commonly considered the workhorse [16]. NBR is a polar elastomer and possesses remarkable resistance to oil absorption due the nitrile content, however, like other elastomers, NBR is not thermally stable. The Elastomer cannot produce a strong char layer when subjected to high temperature and pressure flame. This can be achieved by incorporation of flame retarding or char producing materials. Maamori *et al*. [17] reported that the incorporation of PR along with carbon black in the nitrile rubber improved the thermal properties due to its high strength. PR network exhibits polarity because of hydroxyl group on benzene ring. Both NBR/PR are organic, polar in nature and likely to be miscible in each other. Therefore, blend of NBR/PR (polymer-polymer) without any additional filler will improve ablation resistance and thermal properties of the composite. Due to low cost, the composite could be produced in large quantities and may be employed for retardation of flame or used as thermal insulator for high temperature applications in industries. Due to softer nature, material may be easily molded, shaped and bonded on metallic and non metallic surfaces.

*Corresponding author: noamanulhaq@ciitlahore.edu.pk

In this study, NBR/PR (polymer-polymer) composites were fabricated without any combination of fillers (inorganic or organic) and comparative results were obtained. The effect of PR on ablative performance of the composite was investigated by using an oxy-acetylene flame. Thermal stability and thermal conductivity of NBR/PR composites were characterized by TGA and guard hot plate apparatus. Composition of the ablative composite and post test (ablation) char microstructure were characterized by SEM.

Experimental

Materials

Acrylonitrile butadiene rubber (Kumho KNB 35L) with 34 % acrylonitrile content, supplied by ABF International Corporation limited, Korea. sulphur, zinc oxide and stearic acid were purchased from BDH chemicals USA. Accelerators, tetramethyl thiuriam disulfide (TMTD) and mercapto benzothiazole disulphide (MBTS), and antioxidant trimethyl dihydroquinoline (TMQ) were delivered by Dalian Richon Chemical Co. Ltd., China. Plasticizer, di-octyl phthalate (DOP) was purchased from International petrochemicals (Pvt) Ltd., Pakistan. Phenol formaldehyde resin (Novalac) was supplied by Sumitomo PT Indopherin Jaya Chemicals Indonesia.

Preparation Method

Seven NBR/PR composites having 0, 5, 10, 20, 30, 40 and 50 Phr of PR were blended into the rubber matrix and the fabricated ablative composites were designated N, N5, N10, N20, N30, N40 & N50 in the formulations illustrated in Table 1.

Mixing was carried out in a two-roll mill, operations of kneading and mixing took place on this equipment according to ASTM D15. The ingredients were added according to ASTM D3187-89 as follows:

Elastomer acrylonitrile butadiene rubber (NBR) was passed between the two rolls several times with decreasing the nip between the two rolls to the extent of 0.5-1 mm. Sulfur was added as a vulcanizing agent followed by mixing for homogenization of the materials at room temperature. Then stearic acid and zinc oxide were added as vulcanization activators. After that, di-octyl phthalate (DOP) was added as plasticizers in the NBR matrix. Curing accelerator tetramethylthiuriam disulfide (TMTD), mercapto benzothiazole disulphide (MBTS), and antioxidant trimethyl dihydroquinoline (TMQ) were added. Finally PR was incorporated in NBR. The nip between the rolls was set at 0.8 mm.

Ablation test specimens and specimens for thermal conductivity measurement (ϕ70 mm and 7.0 mm thickness) were fabricated at 1600 psi and 140 °C for 50 minutes on the hot isostatic press.

Characterization and Testing

Ablation Rates

Linear ablation rate, mass ablation rate and percent char were measured according to ASTM E-285-80 [18]. The simplest and cheapest way to perform a test which can partially simulate the severe environment being encountered by an aerodynamic body is based on the use of an oxy-acetylene (OA)torch [8,19]. This device is able to produce both a high temperature flame (up to 3000 °C) and high a heat flux. Figure 1 illustrates the experimental setup ablation testing of NBR/PR composite specimens. The nozzle diameter of the equipment was 2.0 mm, the ablation distance and ablation time was 10 mm and 20 s respectively. Flow rates of oxygen and acetylene were 0.42 m^3/s and 0.31 m^3/s, respectively. The calibration of the power of the flame was performed using a copper slug calorimeter [20] and the heat flux determined was 4120-4450 Kw/m^2. Linear and mass ablation rates were calculated according to the following formula:

$$\text{Linear ablation rate} = \frac{(\text{Initial thickness} - \text{Final thickness})}{\text{Ablation time}} \quad (1)$$

$$\text{Mass ablation rate} = \frac{(\text{Initial mass} - \text{Final mass})}{\text{Ablation time}} \quad (2)$$

Table 1. Composition of the rubber composites

Ingredients	Loading level (phr)						
	N	N5	N10	N20	N30	N40	N50
NBR	100	100	100	100	100	100	100
Zinc oxide	5	5	5	5	5	5	5
Stearic acid	1	1	1	1	1	1	1
DOP	2.5	2.5	2.5	2.5	2.5	2.5	2.5
TMQ	1.0	1.0	1.0	1.0	1.0	1.0	1.0
TMTD	0.5	0.5	0.5	0.5	0.5	0.5	0.5
MBTS	1.0	1.0	1.0	1.0	1.0	1.0	1.0
Sulfur	1.5	1.5	1.5	1.5	1.5	1.5	1.5
Phenolic resin	0	5	10	20	30	40	50

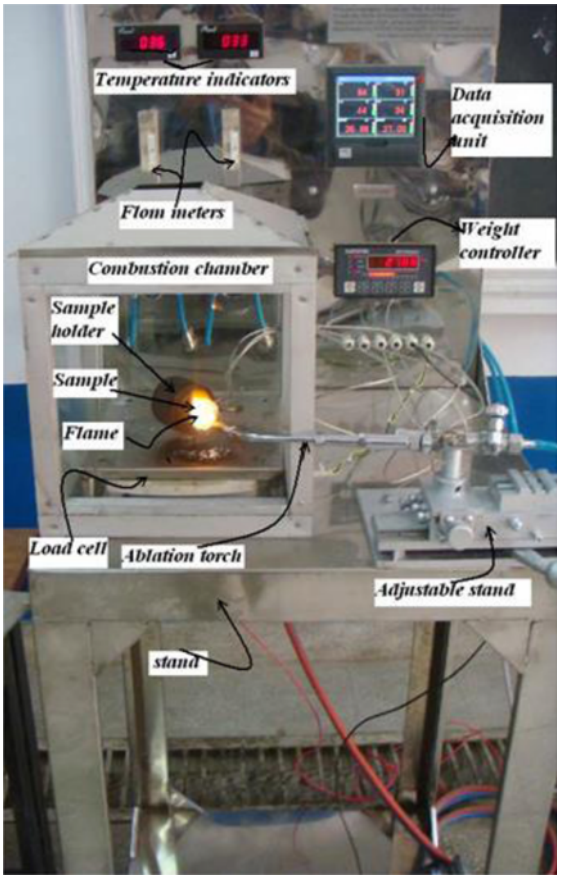

Figure 1. Photograph of oxyacetylene ablation test equipment.

$$\%\ \text{char yield for ablator} = \frac{(\text{Initial mass} - \text{Final mass}) \times 100}{\text{Initial mass}} \tag{3}$$

Morphological Analysis

Scanning Electron Microscopy was performed using SEM, JSM 6490A, Jeol, Japan to characterize homogeneous distribution of ingredients in host matrix, char morphology and pores formation. Energy Dispersive X-ray spectroscopy (EDX) were performed to determine the elemental distribution of the ablative composite.

Thermogravimetric Analyses

Thermaogravimetric analysis (TGA) was performed over the temperature range 20-600 °C on TGA Q50, TA instrument USA at a heating rate of 10 °C/min under nitrogen atmosphere. TGA was performed to find out the thermal stability of the fabricated composites.

Thermal Conductivity

Thermal conductivity is the transfer of heat from one part of a body to another. Thermal conductivity was determined by guarded hot plate apparatus (TP-500) using steady state technique [21] according to ASTM C-177-97. Thermal conductivity K in steady state is given by formula (4).

$$K = \frac{\left(\frac{Q}{A}\right) \times L}{T_u - T_l} \tag{4}$$

where K is thermal conductivity (W/mK) under steady state, T_u is the upper point temperature, T_l is the lower point temperature, Q is the heat flow and A is the cross section area perpendicular to heat flow and L is material thickness.

Density

Sample sheets of 2.0 mm thickness were used to measure density according to ASTM D-4018. Sheets were conditioned at temperature 20±2 °C for one hour before the start of the test. Density was calculated by using the following formula (5).

$$\rho = m_1 \times \frac{\rho 1}{m1 - (m2 - m3)} \tag{5}$$

where $m1$ is mass of sample in air (g), $m2$ is mass of sample+metal wire immersed in paraffin oil (g), $m3$ is mass of metal wire immersed in paraffin oil (g) and $\rho 1$ is density of paraffin oil (g/cm^3).

Results and Discussion

Ablation Rates

The fabricated NBR/PR composites displayed a decrease in linear ablation, mass ablation and increase in char deposition on ablated surface of specimen as illustrated in Figure 2-4. Linear ablation rate, mass ablation rate and char yield rate (CYR) were determined according to the equations (1)-(3).

An increase in blending ratio of PR in NBR from 0 to 50 phr, the linear ablation rate reduced from 97.8 to 21.3 % and mass ablation rate from 65.6 to 26.1 %. Likewise the char content deposition increased from 0.19 to 26.8 %. Since PR is thermally stable and char producing polymeric material

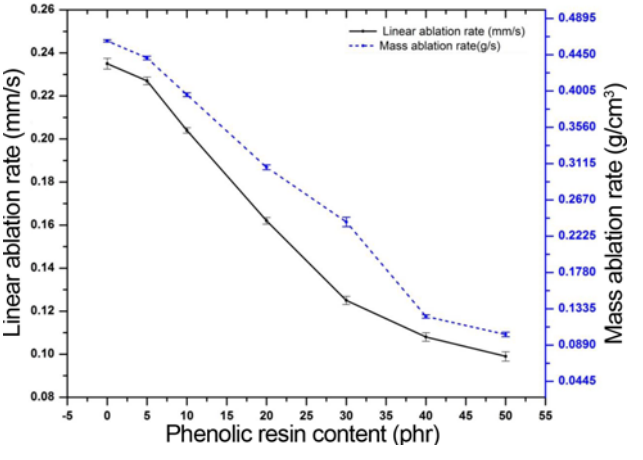

Figure 2. Linear & mass ablation rates of NBR/PR composite.

[22]. The lowest linear/mass ablation rates and highest char yield rate were measured for N50 i.e. 0.102 mm/s and 0.099 g/s respectively. While the highest linear/mass ablation rates and lowest char yield rate were measured for 'N' composite. The formation of char layer on the ablated surface of the specimens was the barrier in reducing linear and mass erosion rates. Poly(p-phenylene-2,6-benzobisoxazole) (PBO) fibers reinforced EPDM has shown the mass loss rate and the erosion rate as low as 0.05 g/s and 0.10 mm/s respectively [5]. Silicone rubber ablative composite filled with silica and carbon fibers displayed linear and mass ablation rates of 0.0472 mm/s and 0.0605 g/s respectively [8]. The excellent

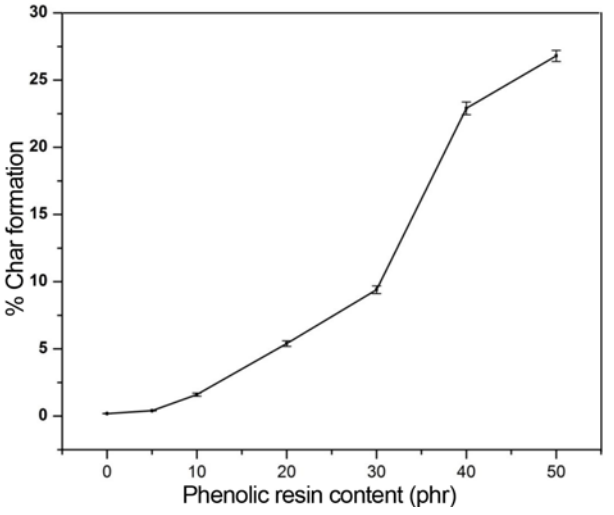

Figure 3. Percentage of char yield NBR/PR composite.

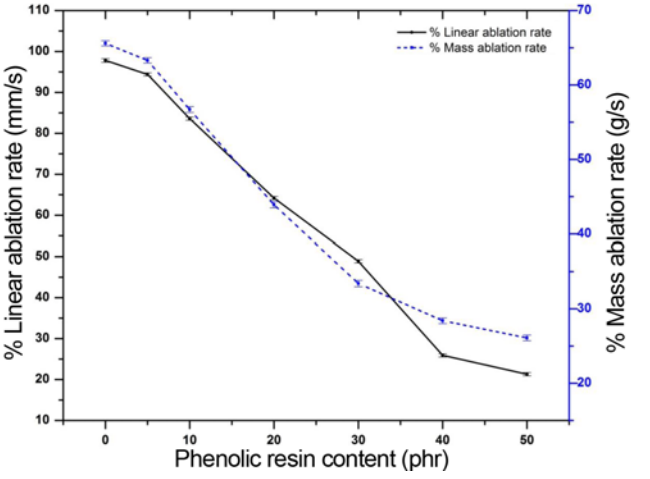

Figure 4. Percentage of linear & mass ablation rates of NBR/PR composite.

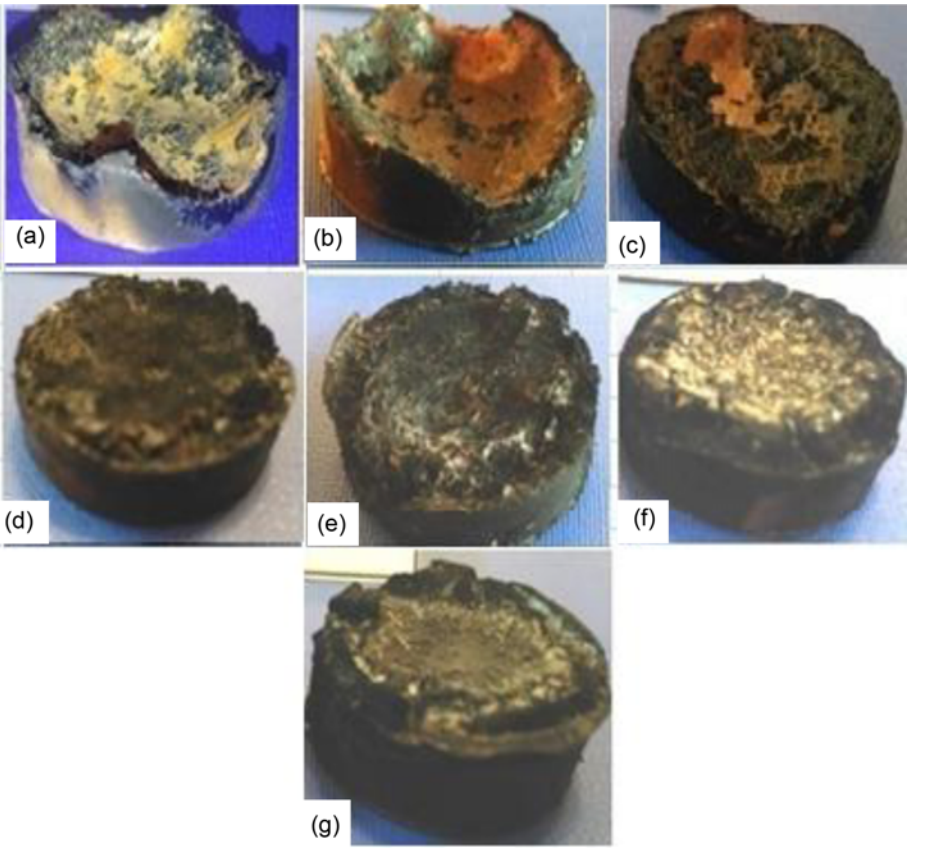

Figure 5. Post burnt specimens' images of NBR/PR composite; (a) N, (b) N5, (c) N10, (d) N20, (e) N30, (f) N40, and (g) N50.

anti-ablative properties by these composites can be attributed to the presence of fillers which have high melting or decomposition temperature. Comparative results for mass ablation were achieved, however, results of linear ablation rate were slightly higher [23] due to the absence of fillers (inorganic/organic) [7]. Figure 5 shows the images of the burnt specimens. The decrement was observed in the center of all specimens due to high temperature, high impact force of oxy-acetylene flame on to the substrate. The erosion was more intense for specimens 'a' and 'b', where char yield rate was negligible due to respective 0 and 5 phr PR content in NBR. Char retention on substrate surface after being subjected to high impact force of oxy-acetylene flame further validates strong interaction between char and substrate and the resin network formation throughout NBR matrix.

Morphological Analysis

Figure 6 depicts SEM micrographs of the composites before ablation. Uniform distribution of the ingredients can be seen in the micrographs. Figure 6(a-e) illustrates that PR showed good dispersion in rubber matrix up to 30 phr and the fabricated composites displayed smooth surfaces. However, when the amount of PR exceeded 30 phr in rubber matrix, formation of an amorphous and brittle phase was seen in the composites as shown in Figure 6(f & g) [24]. This phenomenon in the rubber matrix might be due to phase separation (rubber-resin) during vulcanization. The elemental distribution was determined by energy dispersive X-ray spectroscopy (EDX) and shown in Table 2.

The exposed face of the composite samples shown in Figure 5(a) & (b) underwent severe errosion. It can be clearly seen that the ablated surface are almost without char layer. EDX analysis revealed that the main constituents of deposited material are Carbon, Zinc & Sulfur. Likewise, Figure 5(c) containing relatively more char deposites as compared to (a) and (b). Due to continuous char formation

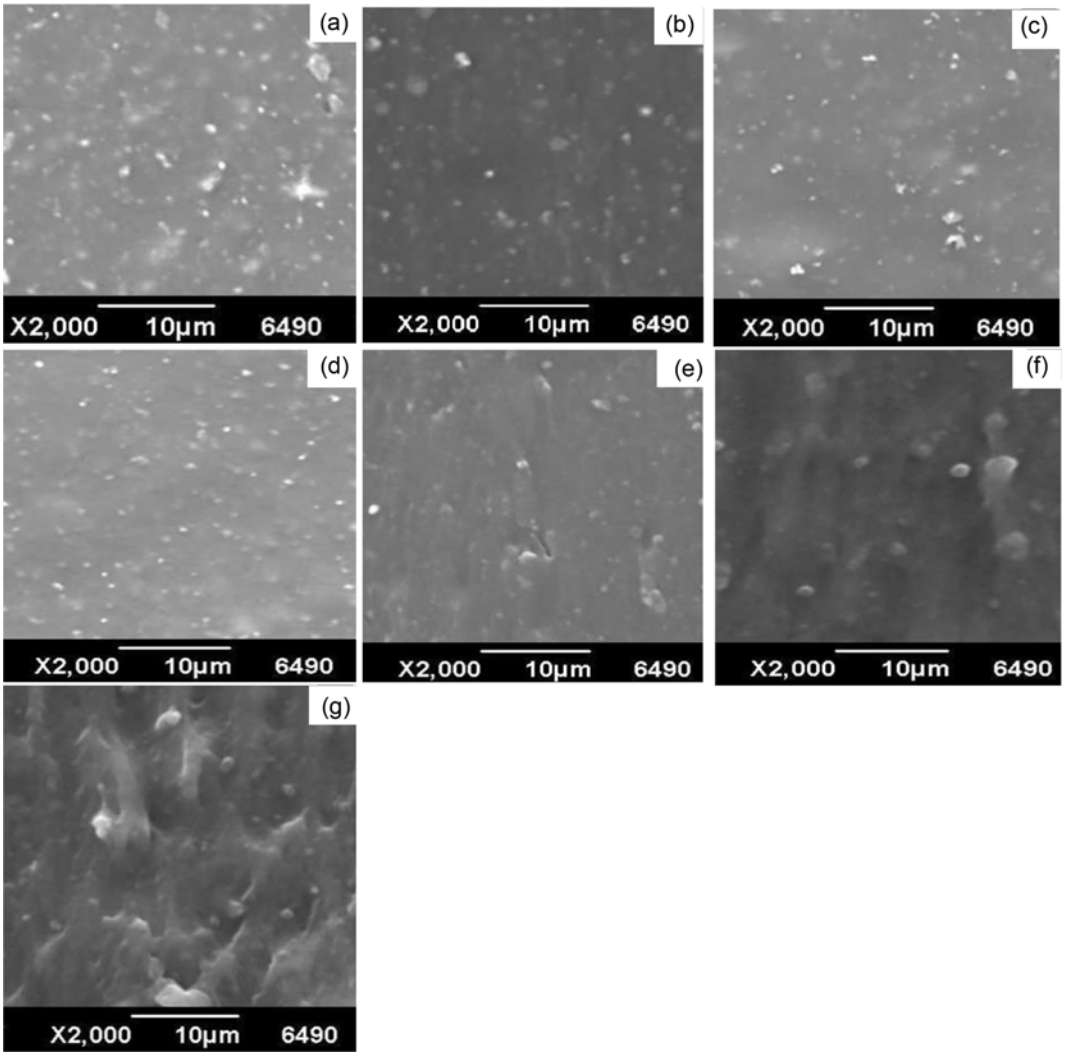

Figure 6. SEM micrographs of Pre-burnt NBR/PR composite; (a) N, (b) N5, (c) N10, (d) N20, (e) N30, (f) N40, and (g) N50.

Table 2. Elemental composition of NBR/PR rubber composite by EDX

Element	Weight (%)						
	N	N5	N10	N20	N30	N40	N50
C	88.67	88.96	88.04	87.88	86.74	86.45	84.8
O	4.57	5.19	5.66	6.37	8.27	9.21	11.05
S	2.37	2.4	1.9	1.56	1.64	1.51	1.44
Zn	4.39	3.45	4.4	4.19	3.35	2.83	2.71

and the subsequent denudation by high speed gases and high temperature flame(oxy-acetylene), remarkable enhancement in terms of linear and mass ablation was noted in (c). Composite specimens shown in Figure 5(d-g) are covered with a thick char layer intact to ablated surface. The reduction in errosion rate is evident from the images.

The char formed as a result of decomposition of NBR/PR matrix could not survived on the surface of ablated specimen against high speed/high temperature oxy-acetylene flame. It further demonstrates that char retention at 5 & 10 phr PR in rubber matrix might not be feasible. The char structure of ablated specimen (c) was loose with wide interconnected pores. Due to the complexity and non-uniformity, it is difficult to obtain accurate dimensions and distribution of pore sizes. Large irregular pores indicate that 20 phr PR in the rubber matrix is not sufficient to form thick char deposits. The loose char structure did not prevent the transfer of external heat and high-temperature gas to the interior to slow down the decomposition rate of the interior of the material, therefore the erosion rate was high. The formation of pores on composite is likely caused by the large amount of pyrolysis gas breaking through the surface of the composite. Pore size reduction in char can be seen in Figure 7(d) with improved ablation performance. Open and loose voids are still visible in char and it is easier for heat to transfer from the surface to the interior. The micro-structural

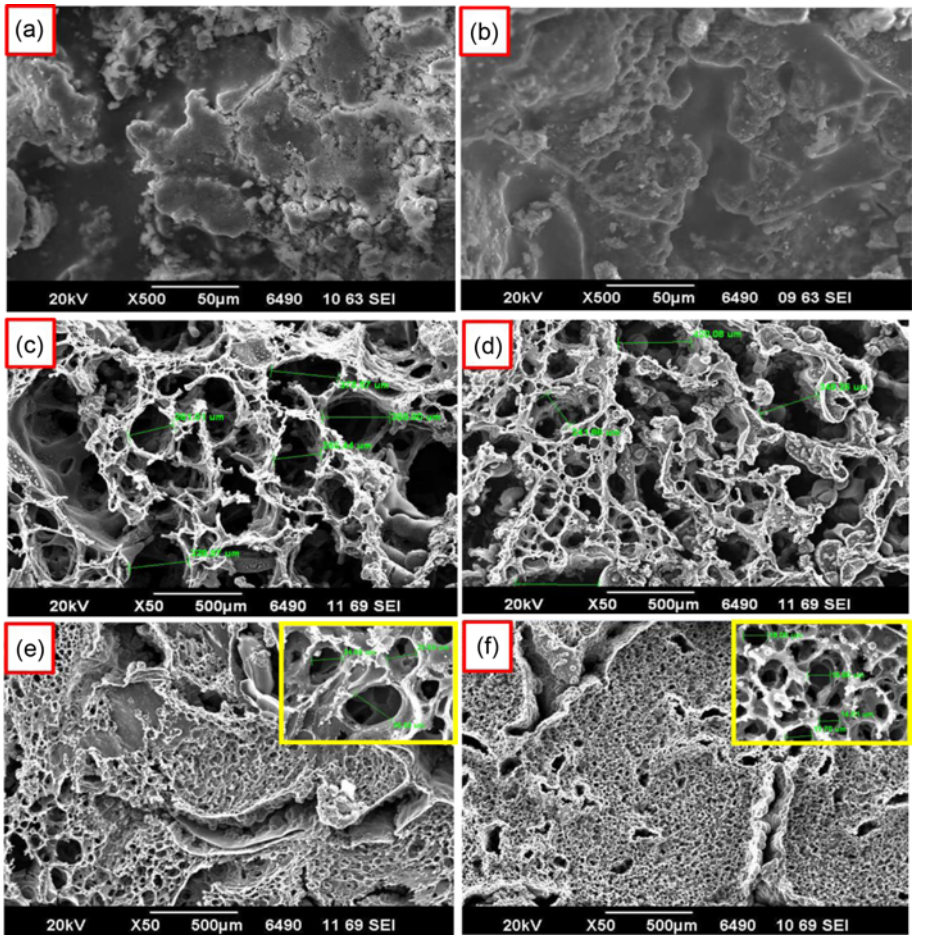

Figure 7. Char layer structure post burnt specimens of NBR/PR composite; (a) N5, (b) N10, (c) N20, (d N30, (e) N40, and (f) N50.

features of char Figure 7(e) imply that increasing PR content resulted in a denser and tougher char. The pores are inter-connected and char layer is almost completely covered with many holes of diameter (22-36 μm). The smaller pore size might be related to high permeability of gases during ablation. In addition to smaller pores, wide pores and cracks can also be seen. Formation of large voids might happen as a result of accumulation of pyrolysis gas in the interior of the material. Char structure was the physical barrier to hinder heat transfer towards the interior of the material which in turn slows down the decomposition of the composite and lowers the linear and mass ablation rates. The char displayed in Figure 7(f) was the most dense and compact [25]. Few wide pores and cracks in ablated surface can also be seen, however, the observed pore sizes for small pores were 14-19 μm. Hence, it could be concluded that the char structure of the NBR/PR composites was the primary factor to improve the ablative performance of the composites [26]. Therefore, from the microscopic viewpoint, the char layer was dense and intact for higher concentration of PR in NBR.

Overall, NBR/PR composite N50 containing 50 phr PR showed the best comprehensive performance interms of linear ablation & mass ablation rates and the char yield rate (26.8 %) [17].

Thermogravimetric Analyses

TGA, derivative thermogravimetry (DTG) curves of neat (un-blended) NBR(N) and phenolic resin (PR) are shown in Figure 8. TGA/DTG curves indicate that PR is more thermally stable than N. Both N and PR display two distinct stages of degradation. For composite specimen N, the DTG peak with first decomposition is observed at 264.7 °C and second decomposition occured at temperature 454.4 °C. First weight and second weight loss for PR were observed at 239.8 °C and 535.9 °C respectively. 5 %, 10 % and major weight losses for PR and N are summarized in Table 3. 5 % weight loss for PR is at lower temperature as compared to N. This loss of weight can be attributed to the evolution of gases trapped in the matrix during the curing reaction [25, 27]. These components include water, formaldehyde and phenol [28]. Correspondingly 10 % weight loss PR at high temperature indicates the stability of PR as compared to N due to linkages formation in polymer structure [29]. The main mass loss of 28.7 % in PR is due to pyrolysis of resin network which took place at temperature range 450-600 °C with evolution of aliphatic, aromatic, hydroxyl, carbonyl, and ether fragments [30]. Likewise for N, the major mass loss (89.1 %) took place at about 350-480 °C. At this temperature range thermal cleavage took place with evolution of acrylonitrile, butenenitrile, ethylene-cyclohexane, hydrogen cyanide, cyano-pentadiene, cyano-hexadiene, dicyano-octadiene [31,32]. The respective residues of 10.9 % and 71.3 % for PR and N left at 600 °C.

Figure 9 depicts TGA and DTG analyses of NBR/PR composites indicating two distinct decomposition stages and thermal stability trend for the composites was observed as N50>N40>N30>N20>N10>N5>N. Table 4 illusrates first and second decompostion temperature. First decomposition in ablative composites N50, N40. N30, N20, N10. N5 and N took place at temperature (T_{max}) 263.8 °C,

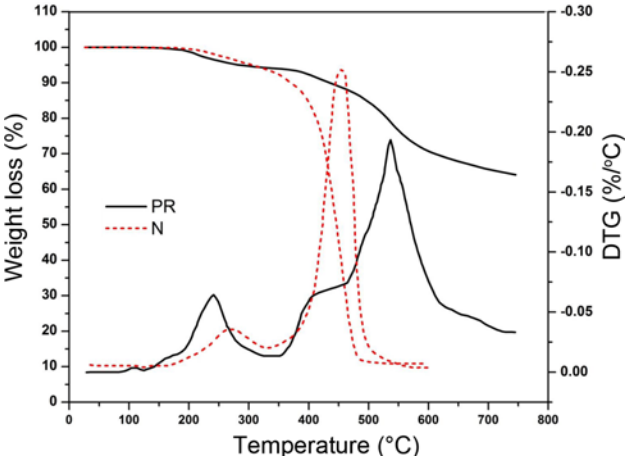

Figure 8. TG & DTG curves of cured unblended NBR (N) and Phenolic Resin (PR).

Table 3. Weight loss data of NBR/PR composite by TGA

Sample ID	5 % weight loss	10 % weight loss	Residue left
PR	274.1 °C	434.2 °C	71.3 %
N	303.9 °C	370.1 °C	10.9 %
N5	292.5 °C	369.9 °C	12.2 °C
N10	284.8 °C	379.8 °C	13.7 °C
N20	282.1 °C	381.7 °C	15.8 °C
N30	267.2 °C	383.5 °C	18.4 °C
N40	265.3 °C	384.2 °C	19.7 °C
N50	256.6 °C	391.9 °C	22.9 °C

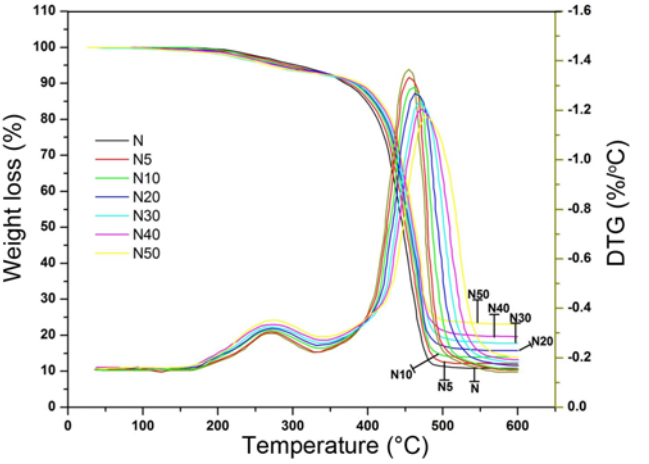

Figure 9. TG & DTG curves of NBR/PR composites.

Table 4. 1st & 2nd decomposition (T_{max}) of NBR/PR composite by TGA

Sample ID	1st decomposition	1st decomposition (T_{max})	2nd decomposition	2nd decomposition (T_{max})
PR	175-295 °C	239.8 °C	460-620 °C	535.9 °C
N	210-330 °C	264.7 °C	375-500 °C	454.4 °C
N5	207-326 °C	272.2 °C	390-500 °C	455.3 °C
N10	202-323 °C	271.2 °C	397-505 °C	462.5 °C
N20	195-315 °C	270 °C	405-515 °C	465.1 °C
N30	191-313 °C	268.5 °C	415-520 °C	471.2 °C
N40	187-306 °C	266.1 °C	422-527 °C	474.1 °C
N50	180-300 °C	263.8 °C	435-540 °C	477.7 °C

266.1 °C, 268.5 °C, 270 °C, 271.2 °C, 272.2 °C and 274.7 °C respectively. First degradation peak mainly corresponds to the formation of by-product of sulfur vulcanization and stearic acid, water molecule, volatile matter etc. [28,33]. Correspondingly the second decomposition for composites N50, N40. N30, N20, N10. N5 and N took place around temperature (T_{max}) 477.7 °C, 474.1 °C, 471.2 °C, 465.1 °C, 462.5 °C, 455.3 °C and 454.4 °C respectively. At low temperature (125-250 °C) the NBR/PR composites were stable relatively with an initial weight loss of 2-4 % due to evolution of trapped water molecules and gasses formed during curing of phenolic resin in the matrix material [25]. The weight loss up to 380 °C was due to plasticizer (DOP) evaporation [31]. Deterioration was more intense at temperature range 365-480 °C due to pyrolysis of elastomer and resin network and 55 to 65 % weight loss was observed. Generally composites with lesser percentage of PR exhibits lesser stability at high temperature and low residues percentage. Overall specimen N50 containing 50 Phr of PR was the most stable composite by 22-23 °C than specimen N (without PR). Residues of 22.9, 19.7, 18.4, 15.8, 13.7, 12.2, 10.9 for composites N50, N40, N30, N20, N10, N5 and N respectively left at 600 °C [34]. Polyimide blended NBR has displayed 8-9 °C improvement in thermal stability and 36% char residue [35]. This demonstrates that heat was transferred very slowly and the slower heat transfer also indicated that more time was required to reach the degradation temperature of the composite. This partly contributed to reduce material loss during ablation and TGA. The improvement in thermal degradation stability and final char residues of composite as compared to neat rubber may be attributed to the uniform rubber-resin blending [34].

Thermal Conductivity

Values of thermal conductivities are of the order N50 > N40 > N30 > N20 > N10 > N5 > N as depicted in Figure 10. A slight increase in thermal conductivity was observed as the loading of PR was increased in Elastomer [36,37]. Composite

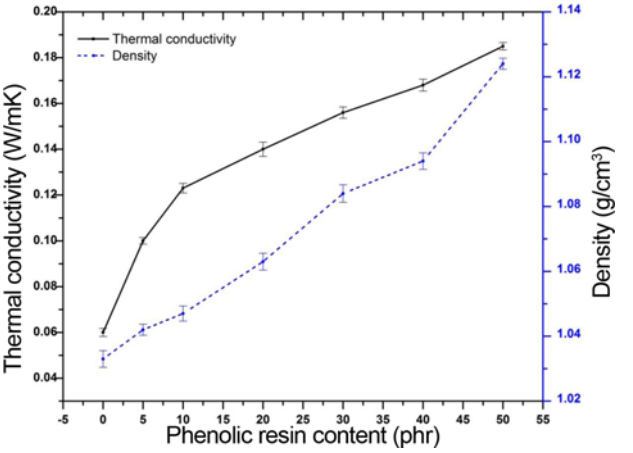

Figure 10. Thermal conductivity vs density of NBR/PR composites.

N50 containing 50 phr PR exhibits the highest density 1.124 g/cm^3 and the highest thermal conductivity value 0.185 W/mK. Thermal conductivity of composite sample N (without PR) has the lowest value 0.07 W/mK. Thermal conductivities of EPDM matrix, aramid fiber/composites and PBO fiber/composites are 0.218, 0.254, and 0.247 (W/mK), respectively [5]. The formation of Phenolic resin network is mainly responsible for thermal conduction through the composite [38]. 0.0023 W/mK was an average rise in thermal conductivity per phr increase of PR content in composite. Ablative composites with low thermal conductivity is primarily more important and more desirable than maintaining its mechanical properties [39]. The slight increase in thermal conductivity of NBR/PR composites indicates that PR is an excellent thermal insulating material as compared to other insulating materials [36,38].

Conclusion

In this work, ablative and thermal performances of phenolic resin (PR) filled acrylonitrile butadiene rubber (NBR) were analyzed using oxyacetylene test. NBR/PR composites were prepared by means of a two-roll mixer. Uniform distribution of PR could be achieved by means of two-roll mixer. The ablation test results revealed that addition of PR significantly decreased the erosion rates. It is also observed that char layer produced by PR acted as a thermal barrier and mechanical stabilizer which in turn hold and prevent material denudation. Thermal decomposition PR filled composites took place at high temperature when compared to unfilled composites. The composite showed slight increase in thermal conductivity value. Over all, NBR/PR composites, the specimen N50 with highest PR content (50 phr) has shown the best comprehensive performance in terms of linear ablation rate, mass ablation rate and thermal stability. This specimen exhibited highest char yield with small sized pores. Thermal conductivity value for this specimen was slightly higher.

References

1. G. Pulci, J. Tirillò, F. Marra, F. Fossati, C. Bartuli, and T. Valente, *Compos. Pt. A-Appl. Sci. Manuf.*, **41**, 1483 (2010).
2. Y. Jiang, X. Zhang, J. He, L. Yu, and R. Yang, *Polym. Degrad. Stabil.*, **96**, 949 (2011).
3. M. Natali, M. Monti, J. M. Kenny, and L. Torre, *Compos. Pt. A-Appl. Sci. Manuf.*, **42**, 1197 (2011).
4. T. S. Najim, A. M. Naji, and M. M. Barbooti, *Leonardo Electronic Journal of Practices and Technologies*, **1**, 34 (2008).
5. G. Gao, Z. Zhang, X. Li, Q. Meng, and Y. Zheng, *Polym. Bull.*, **64**, 607 (2010).
6. L. C. Carwile and H. J. Hoge, *Rubber Chem. Technol.*, **39**, 126 (1966).
7. D. Yang, W. Zhang, B. Jiang, and Y. Guo, *Compos. Pt. A-Appl. Sci. Manuf.*, **44**, 70 (2013).
8. D. Yang, W. Zhang, and B. Jiang, *Ceramics International*, **39**, 1575 (2013).
9. L. Yang, *Procedia Engineering*, **43**, 552 (2012).
10. H.-T. Chu, S.-M. Sheu, and J.-H. Chou, *Journal of Propulsion and Power*, **27**, 1108 (2011).
11. A. S. Deuri, A. K. Bhowmick, R. Ghosh, B. John, T. Sriram, and S. De, *Polym. Degrad. Stabil.*, **21**, 21 (1988).
12. C. Bhuvaneswari, S. Kakade, V. Deuskar, A. Dange, and M. Gupta, *Defence Sci. J.*, **58**, 94 (2008).
13. Y. Guan, L.-X. Zhang, L.-Q. Zhang, and Y.-L. Lu, *Polym. Degrad. Stabil.*, **96**, 808 (2011).
14. V. L. da Cunha Lapa, L. L. Y. Visconte, J. E. de Sena Affonso, and R. C. R. Nunes, *Polymer Testing*, **21**, 443 (2002).
15. A. Shojaei and M. Faghihi, *Mater. Sci. Eng.: A*, **527**, 917 (2010).
16. D. Mackey and A. H. Jorgensen, *Kirk-Othmer Encyclopedia of Chemical Technology*, **21**, 230 (2001).
17. M. H. Al-Maamori, A. A.-A. Al-Zubaidi, and A. A. Subeh, *Int. J. Mater. Sci. Appl.*, **4**, 43 (2015).
18. E. ASTM, *Annual Book of ASTM Standards*, **15** (2008).
19. A. R. Bahramian and M. Kokabi, *Journal of Hazardous Materials*, **166**, 445 (2009).
20. A. Standard, *Annual Book of ASTM Standards, Space Simulation; Aerospace and Aircraft; Compos. Mater*, 15 (2008).
21. R. Oram and E. Wolff in "Advances in Cryogenic Engineering Materials", p.349, Springer, 1998.
22. J. Chen, W. Wu, T. Zhou, W. Fan, and Q. Lu, *J. Macromol. Sci.®, Part B: Phys.*, **50**, 111 (2010).
23. N. Iqbal, S. Sagar, M. B. Khan, and H. M. Rafique, *Polym. Eng. Sci.*, **54**, 255 (2014).
24. D. Setua, M. Shukla, V. Nigam, H. Singh, and G. Mathur, *Polym. Compos.*, **21**, 988 (2000).
25. M. Natali, M. Monti, D. Puglia, J. M. Kenny, and L. Torre, *Compos. Pt. A-Appl. Sci. Manuf.*, **43**, 174 (2012).
26. J. Wang, L. J. Feng, A. Lei, A. J. Yan, and X. J. Wang, *J. Appl. Polym. Sci.*, **125**, 505 (2012).
27. B. John, D. Mathew, B. Deependran, G. Joseph, C. R. Nair, and K. Ninan, *J. Mater. Sci.*, **46**, 5017 (2011).
28. C. Fyfe, M. McKinnon, A. Rudin, and W. Tchir, *J. Polym. Sci.: Polym. Lett. Ed.*, **21**, 249 (1983).
29. A. Konp and L. Pilato, "Phenolic Resins, Chemistry, Application and Performance", Springer-Verlag, Berlin, 1985.
30. A. Knop and L. A. Pilato in "Phenolic Resins", p.147, Springer, 1985.
31. J. A. Hiltz, *J. Anal. Appl. Pyrol.*, **55**, 135 (2000).
32. A. Pappa, K. Mikedi, A. Agapiou, S. Karma, G. Pallis, M. Statheropoulos, and M. Burke, *J. Anal. Appl. Pyrol.*, **92**, 106 (2011).
33. A. S. Deuri and K. Bhowmick, *J. Therm. Anal.*, **32**, 755 (1987).
34. C. Zhang, K. Pal, J. U. Byeon, S. M. Han, and J. K. Kim, *J. Appl. Polym. Sci.*, **119**, 2737 (2011).
35. M. Alneamah and M. Almaamori, *Int. J. Mater. Chem.*, **5**, 1 (2015).
36. T.-E. Kim, J. C. Bae, K. Y. Cho, Y.-G. Shul, and D. H. Riu, *Asian J. Chem.*, **25**, 5625 (2013).
37. H. Ebadi-Dehaghani and M. Nazempour, "Thermal Conductivity of Nanoparticles Filled Polymers", INTECH Open Access Publisher, 2012.
38. R. Patton, C. Pittman, L. Wang, J. Hill, and A. Day, *Compos. Pt. A-Appl. Sci. Manuf.*, **33**, 243 (2002).
39. J. K. Park, D. Cho, and T. J. Kang, *Carbon*, **42**, 795 (2004).